

Improved RF Measurements of SRF Cavity Quality Factors

J.P. Holzbauer, C. Contreras[†], Y. Pischalnikov, D. Sergatskov, W. Schappert

*Fermi National Accelerator Laboratory
P.O. Box 500, Batavia, IL 60510, USA*

*[†]Michigan State University
220 Trowbridge Rd, East Lansing, MI 48824*

Abstract

SRF cavity quality factors can be accurately measured using RF-power based techniques only when the cavity is very close to critically coupled. This limitation is from systematic errors driven by non-ideal RF components. When the cavity is not close to critically coupled, these systematic effects limit the accuracy of the measurements. The combination of the complex base-band envelopes of the cavity RF signals in combination with a trombone in the circuit allow the relative calibration of the RF signals to be extracted from the data and systematic effects to be characterized and suppressed. The improved calibration allows accurate measurements to be made over a much wider range of couplings. Demonstration of these techniques during testing of a single-spoke resonator with a coupling factor of near 7 will be presented, along with recommendations for application of these techniques.

Keywords:

Superconducting RF

PACS: 85.25.Am, 84.40.Dc

*Operated by Fermi Research Alliance, LLC under Contract No. De-AC02-07CH11359 with the United States Department of Energy.

Email address: jeremiah@fnal.gov (J.P. Holzbauer)

1. Power-based RF Cavity Quality Factor Measurements

Cavity quality factors are typically measured using a circuit like that shown in Figure 1 [1]. The cavity is driven by an amplifier through a transmission line. A directional coupler separates the forward and reflected waves inside the transmission line. A probe monitors the cavity field.

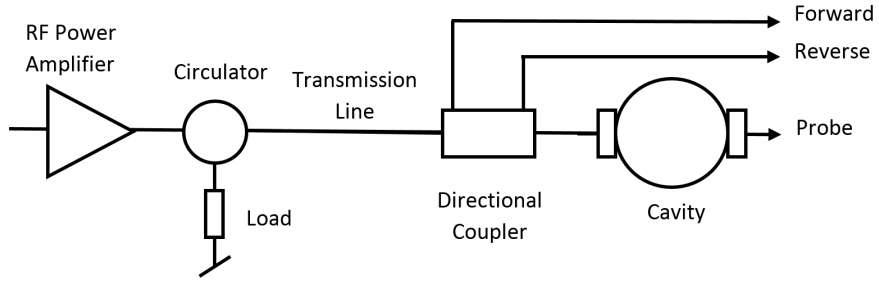


Figure 1: Traditional SRF cavity RF circuit.

The power of the forward, reverse and transmitted waves during steady state operation on resonance in can be combined with measurements of the cavity decay time to determine cavity quality factors if the cavity is close to critically coupled.

The cavity frequency and decay time can be combined to determine the loaded quality factor, Q_L :

$$Q_L = \omega \tau_{Power}. \quad (1)$$

The reduced cavity coupling factor, β^* , can be determined from the cavity reflection coefficient:

$$\beta^* = Q_{Ext}^{-1} (Q_0^{-1} + Q_T^{-1})^{-1} = \frac{\sqrt{P_{Forward}^{SS}} \pm \sqrt{P_{Reverse}^{SS}}}{\sqrt{P_{Forward}^{SS}} \mp \sqrt{P_{Reverse}^{SS}}} \quad (2)$$

where SS represents Steady State, Q_0 is the cavity intrinsic quality factor,

and Q_{Ext} is the input coupler quality factor. The top signs are for an over-coupled cavity, and the bottom signs are for an under-coupled cavity.

The cavity field probe coupling can then be determined from Q_L , β^* , and the steady state forward and probe power measurements as follows:

$$Q_T = \frac{P_{Reactive}}{P_{Probe}} = \frac{4Q_L}{1 + \beta^{*-1}} \frac{P_{Forward}^{SS}}{P_{Probe}^{SS}}. \quad (3)$$

Finally, the intrinsic quality factor, Q_0 , can be calculated from the above quantities as follows:

$$Q_0 = \frac{Q_T Q_L (1 + \beta^*)}{Q_T - Q_L (1 + \beta^*)}. \quad (4)$$

The cavity gradient can be determined from the cavity probe coupling, probe power, cavity impedance (R/Q), and effective length, L_{Eff} :

$$E_{Acc} = \frac{\sqrt{Q_T P_{Probe} (R/Q)}}{L_{Eff}}. \quad (5)$$

Several systematic effects can bias such measurements [2]:

1. Impedance mismatches between the circulator and the transmission line can reflect reverse energy back into the forward wave. During the decay this can lead to a non-zero forward wave which can interfere constructively or destructively with the cavity field, lengthening or shorting the cavity decay time.
2. Cross-talk (directivity) in the directional coupler used to separate the forward and reflected waves can cross-contaminate the forward and reflected signals leading to systematic biases in the cavity coupling measurement.

2. Improving RF-based Quality Factor Measurements

Circulator mismatches and imperfect directivity can be measured by:

1. Inserting a variable length transmission line (trombone) in the circuit between the directional coupler and the cavity as shown schematically in Figure 2 and

- Recording the complex cavity baseband waveforms for a range of cavity detuning values as the length of the trombone is systematically varied over a wavelength at the cavity frequency.

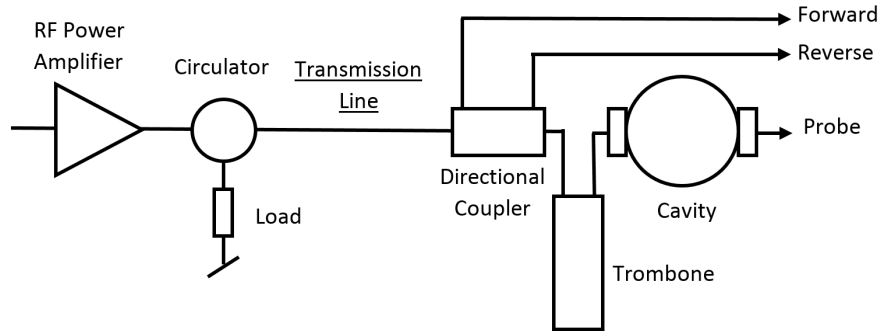


Figure 2: Modified SRF cavity RF circuit including trombone between directional coupler and cavity. This was the RF circuit used during the measurements presented.

Changing the length of the trombone will change the phase with respect to the cavity field of energy reflected by the circulator from the reverse wave back into the forward wave. As the trombone length is swept over a wavelength, the phase of this energy should sweep through 4π . This phase change should modulate the measured decay time of the cavity/waveguide system sinusoidally through 2 complete cycles. The magnitude and phase of the modulation can be used to determine the complex circulator reflection coefficient which can be used in turn to correct the measured decay time for circulator impedance mismatches.

Changing the trombone length will also change the relative phases of the forward, reverse with respect to the cavity field. As the length of the trombone is swept over a wavelength, the forward/probe and reverse/probe phase will sweep from 0 through 2π in opposite directions. If the phase of the RF signals in addition to the magnitude is recorded during the trombone sweep, the complex directivity of the coupler can be determined and used to suppress cross-contamination of the two signals offline.

The cavity signals can then be corrected for these two systematic effects,

improving the accuracy of the decay time and cavity coupling measurements.

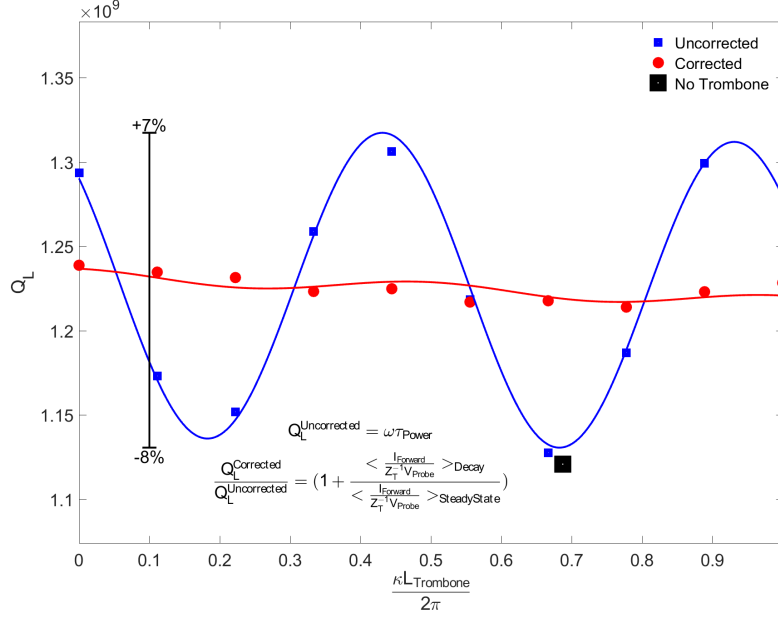


Figure 3: Variation of Loaded Quality Factor Q_L with trombone length (Blue Squares). The Q_L measured without the trombone in the circuit (Black Square) agrees with these measurements. Using directivity-corrected powers, the measured Q_L can be corrected (Red Circles) to give results mostly independent of trombone position.

The technique is illustrated using data recorded from a 325 MHz single spoke resonator [3, 4] installed in the Fermilab STC [5] operating at 2K with and a nominal gradient of 5 MV/m. The RF circuit was modified by installing a trombone between the directional coupler and the cavity. The length of the trombone was systematically varied over one wavelength ($c/325\text{MHz}$) in 10 steps. At each step of the trombone, the phase of the PLL locking the drive frequency to the cavity resonance frequency was varied in 7 steps between -45° and 45° while the complex baseband RF signals were recorded using a digital RF control system provided by the Fermilab AD/LLRF group [6] for an interval of 10 seconds. During each recording the generator power was shut off after approximately 7 seconds, allowing the cavity to decay.

For comparison, a control sample was recorded without the trombone in the circuit while the lock phase was varied over the same range.

3. Cavity Decay Measurements

The blue and red points in Figure 3 respectively compare the loaded cavity quality factor, Q_L , as a function of trombone position before and after correction for impedance mismatches at the circulator. The uncorrected measurements were multiplied by the following factor to account for non-zero forward power during the decay to obtain the corrected measurements. Remaining linear trend in the data is likely from additional attenuation in the trombone.

$$\frac{Q_L^{Corrected}}{Q_L^{Uncorrected}} = \text{Re} \left\{ 1 + \frac{\left\langle \frac{I_{Forward}^{Cavity}}{Z_T^{-1} V_{Cavity}} \right\rangle_{Decay}}{\left\langle \frac{I_{Forward}^{Cavity}}{Z_T^{-1} V_{Cavity}} \right\rangle_{SS}} \right\} \quad (6)$$

The uncorrected measurements (blue squares) vary sinusoidally by up to 8% over two cycles as the length of the trombone is varied over a wavelength while the corrected measurements (red circles) are much less sensitive to trombone length.

The black square shows the equivalent measurement with no trombone in the circuit. The value is consistent with the value expected from the trombone measurements when the phase length of the waveguide is the same.

4. Measuring and Correcting Directivity

Cross-contamination of the forward and reverse signals extracted by the directional coupler can lead to significant systematic biases in the determination of the cavity coupling if the cavity is not close to critically coupled.

The measurement of the forward and reverse waves by the directional coupler can be modelled by the product of a trombone dependent phase delay and a linear mixing matrix representing cross-talk (directivity) in the coupler:

$$\begin{bmatrix} I_{Forward}^{DC} \\ I_{Reverse}^{DC} \end{bmatrix} = \begin{bmatrix} G_F & \epsilon_F \\ \epsilon_R & G_R \end{bmatrix} \begin{bmatrix} e^{i\kappa L_{Trom}} & 0 \\ 0 & e^{-i\kappa L_{Trom}} \end{bmatrix} \begin{bmatrix} I_{Forward}^{Cavity} \\ I_{Reverse}^{Cavity} \end{bmatrix}. \quad (7)$$

The derivatives of the measured forward/probe signal ratio and measured reflected/probe signal ratio with respect to changes in detuning are related as follows.

$$r_D(L_{Trom}) = \frac{\frac{\partial}{\partial \delta} \frac{I_{Reverse}^{DC}}{Z_T^{-1} V_{Cavity}}}{\frac{\partial}{\partial \delta} \frac{I_{Forward}^{DC}}{Z_T^{-1} V_{Cavity}}} = -e^{-2i\kappa L_{Trom}} \frac{G_R - \epsilon_R e^{2i\kappa L_{Trom}}}{G_F - \epsilon_F e^{-2i\kappa L_{Trom}}} \quad (8)$$

$$\approx \frac{\epsilon_R}{G_F} - e^{-2i\kappa L_{Trom}} \frac{G_R}{G_F} + \frac{\epsilon_F}{G_F} e^{-4i\kappa L_{Trom}} \quad (9)$$

The relative complex gain of the forward and reverse waves and cross-contamination coefficients can be determined by Fourier transforming this ratio with respect to the length of the trombone:

$$R_D(n) = -\sqrt{\frac{\kappa}{2\pi}} \int_0^{\frac{2\pi}{\kappa}} dL_{Trom} e^{2i\kappa n L_{Trom}} r_D(L_{Trom}). \quad (10)$$

The complex elements of the mixing matrix are then determined up to a single overall complex gain factor, G_F^{-1} :

$$\frac{\epsilon_F}{G_F} = R_D(-4); \quad \frac{G_R}{G_F} = -R_D(-2); \quad \frac{\epsilon_R}{G_F} = R_D(0). \quad (11)$$

The overall gain factor can be determined by requiring the inverse transfer functions sum to unity.

$$\begin{bmatrix} T_{P/F}^{-1} \\ T_{P/R}^{-1} \end{bmatrix} = G_F^{-1} \begin{bmatrix} e^{i\kappa L_{Trom}} & 0 \\ 0 & e^{-i\kappa L_{Trom}} \end{bmatrix} \begin{bmatrix} 1 & \frac{\epsilon_F}{G_F} \\ \frac{\epsilon_R}{G_F} & G_R/G_F \end{bmatrix}^{-1} \begin{bmatrix} \frac{I_{Forward}^{DC}}{Z_T^{-1} V_{Cavity}} \\ \frac{I_{Reverse}^{DC}}{Z_T^{-1} V_{Cavity}} \end{bmatrix}; \quad (12)$$

$$T_{P/F}^{-1} + T_{P/R}^{-1} = 1. \quad (13)$$

This linearized procedure can be iterated several times to find a solution of original rational relationship.

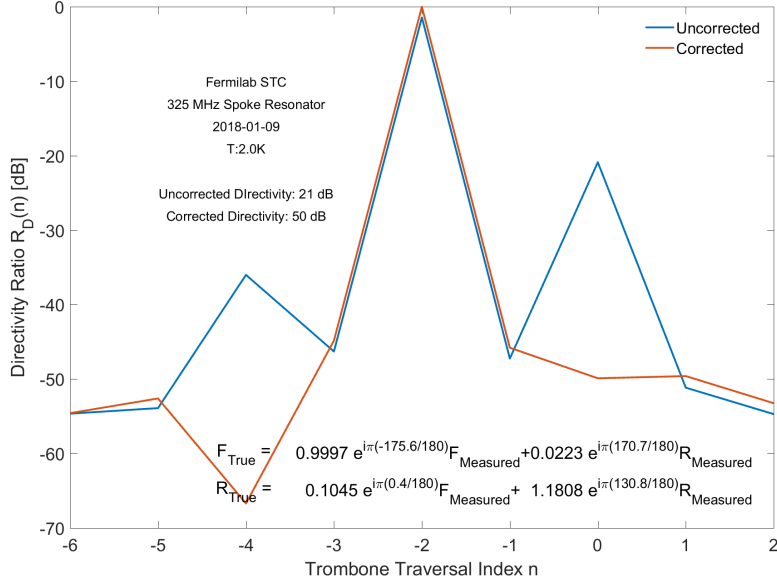


Figure 4: Directivity determination before and after correction factor applied.

Figure 4 compares the transformed derivative ratio measured for the 325 MHz cavity under test before and after directivity determination and correction. As would be expected from the equations, the uncorrected ratio shows a large peak at -2 corresponding to the coefficient ratio G_R/G_F and smaller peaks at -4 and 0 corresponding to the coefficient ratios ϵ_F/G_F and ϵ_R/G_F . Before correction the directivity is 21 dB. Following offline correction, the directivity improves to 50 dB giving much better separation and relative calibration of the forward and reflected waves.

5. Cavity Coupling and Inverse Transfer Functions

The response of a cavity resonance can be modeled as a RLC oscillator driven from a transmission line at an angular drive frequency, ω_{Drive} , as shown schematically in Figure 5.

With the following substitutions:

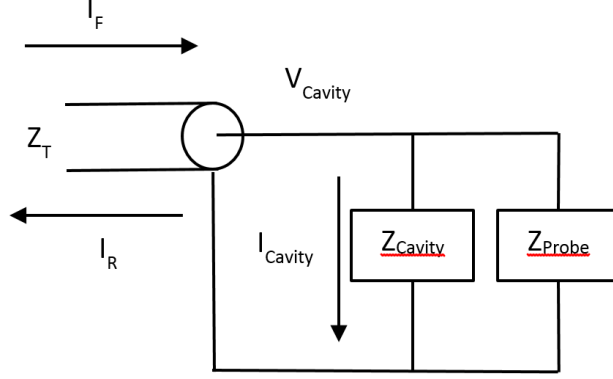


Figure 5: Cavity circuit model including probe coupler.

$$Z_0 = \sqrt{\frac{L}{C}} \equiv \frac{R}{Q}; \quad \omega_0 = \frac{1}{\sqrt{LC}}; \quad \beta^{-1} = \frac{Z_T}{R_0}; \quad (14)$$

$$\omega_{\text{Baseband}} = \omega - \omega_{\text{Drive}}; \quad \delta = \omega_0 - \omega_{\text{Drive}}; \quad \omega_T = \frac{Z_0 \omega_{\text{Drive}}}{2Z_T} \equiv \frac{\omega_{1/2}}{1 + \beta^{-1}}; \quad (15)$$

the cavity impedance can be written in terms of a dimensionless coupling factor β , base-band modulation frequency ω_{Baseband} , detuning δ , and reduced half bandwidth ω_T :

$$\frac{Z_T}{Z_{\text{Cavity}}} = \frac{Z_T}{R_0} + i \frac{Z_T}{Z_0} \left(\frac{\omega}{\omega_0} - \frac{\omega_0}{\omega} \right) \quad (16)$$

$$\approx \beta^{-1} + i \frac{\omega_{\text{Baseband}} - \delta}{\omega_T}. \quad (17)$$

The complex base-band envelopes of the forward and reverse waves at the cavity and the cavity voltage are then related by the following inverse transfer functions:

$$T_{P/F}^{-1} = \frac{I_{\text{Forward}}^{\text{Cavity}}}{Z_T^{-1} V_{\text{Cavity}}} = \frac{1}{2} \left(1 + \beta^{*-1} + i \frac{\omega - \delta}{\omega_T} \right) \quad (18)$$

$$T_{P/R}^{-1} = \frac{I_{Reverse}^{Cavity}}{Z_T^{-1} V_{Cavity}} = \frac{1}{2} \left(1 - \beta^{*-1} - i \frac{\omega - \delta}{\omega_T} \right) \quad (19)$$

$$\beta^{*-1} = \frac{Z_T}{R_0} + \frac{Z_T}{Z_{Probe}}. \quad (20)$$

The sum of the inverse transfer functions adds to unity while the derivatives with respect to detuning are equal and opposite.

$$T_{P/F}^{-1} + T_{P/R}^{-1} = 1 \quad (21)$$

$$\frac{\partial T_{P/F}^{-1}}{\partial \delta} + \frac{\partial T_{P/R}^{-1}}{\partial \delta} = 0 \quad (22)$$

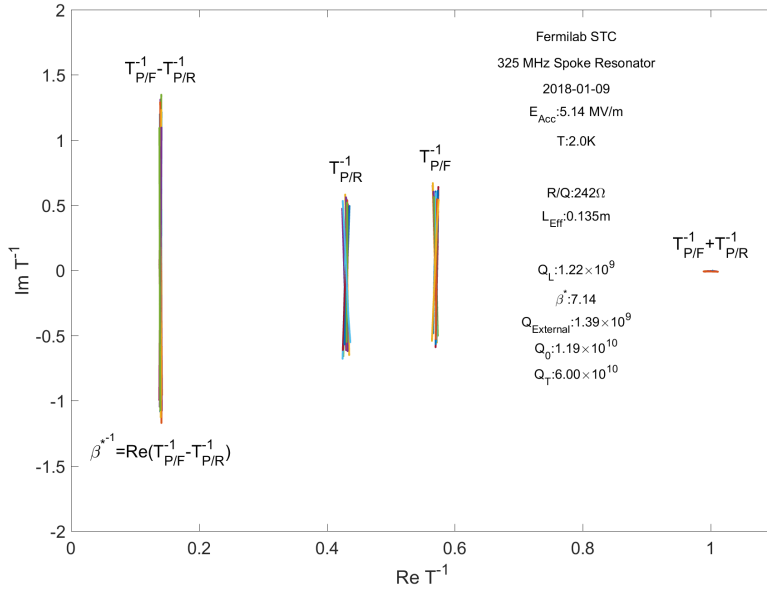


Figure 6: Measured Inverse Transfer Functions and derived quantities. Each color represents a different trombone position.

These constraints can be used to determine the relative complex gain of the three cavity RF signals from the data itself.

The real and imaginary components of the difference of the two transfer functions yield the inverse cavity coupling and detuning respectively:

$$T_{P/F}^{-1} - T_{P/R}^{-1} = \beta^{*-1} + i \frac{\omega - \delta}{\omega_T}. \quad (23)$$

This allows the inverse coupling to be determined directly from the calibrated inverse transfer functions with no ambiguity whether the cavity is over or under-coupled.

Following correction for directivity and calibration, the cavity inverse transfer functions can be determined from the complex steady state ratios of the forward/probe and reverse/probe signals.

The inverse transfer functions measured for the 325MHz cavity under test operating at 2K are plotted in the complex plane in Figure 6.

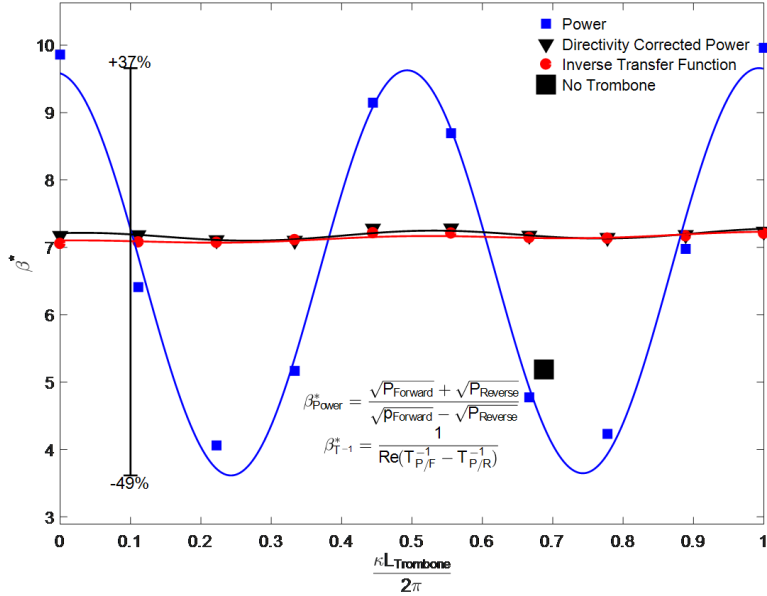


Figure 7: Measured β^* via Power measurements versus trombone angle with uncorrected signals (Blue Squares) and directivity-corrected signals (Black Triangles) compared to directivity-corrected Transfer Functions (Red Circles). β^* measured without trombone (Black Square) agrees with trombone scan data.

The multiple vertical lines for each inverse transfer function represent independent measurements of the two inverse transfer functions as the lock phase is varied between -45° and 45° at the each of the different trombone lengths. As the lock is varied the detuning of the cavity changes and the transfer functions sweep along a vertical line in the complex plane. As expected both inverse transfer functions show little sensitivity to changes in the trombone length.

The inverse cavity coupling can be determined directly from the real component of the difference between the two inverse transfer functions:

$$\text{Re}\{T_{P/F}^{-1} - T_{P/R}^{-1}\} = \beta^{*-1}. \quad (24)$$

The blue and black points in Figure 7 respectively compare the cavity coupling, β^* , as a function of trombone position both before and after the cavity

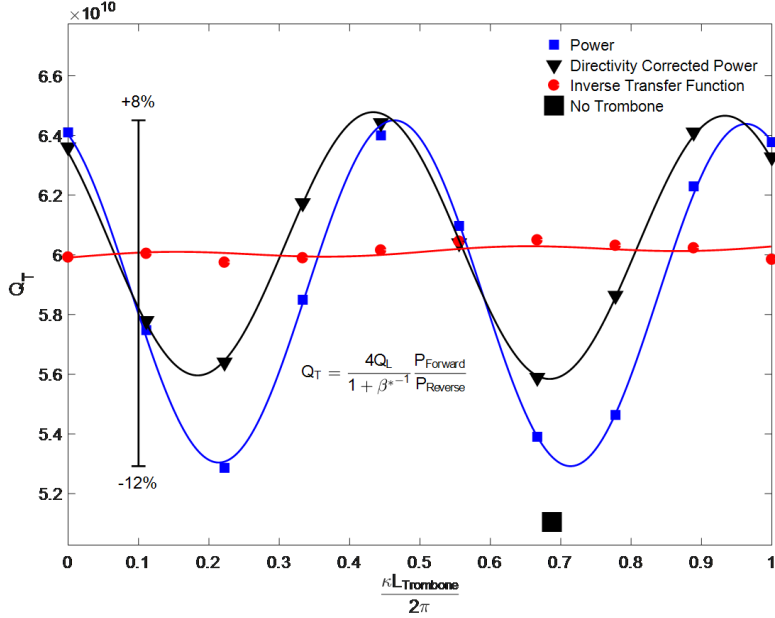


Figure 8: Measured Q_T via Power measurements versus trombone angle with uncorrected signals (Blue Squares) and directivity-corrected signals (Black Triangles) compared to directivity-corrected Transfer Functions (Red Circles). Q_T measured without trombone (Black Square) agrees with trombone scan data.

power measurements were corrected for directivity. The red points show the inverse cavity coupling determined using the inverse transfer functions.

The blue and black points in Figure 8 respectively compare the cavity field probe coupling, Q_T , as a function of trombone position both before and after the cavity power measurements were corrected for directivity. The red points show the inverse cavity coupling determined using the inverse transfer functions.

The uncorrected power measurements (blue) vary sinusoidally by up to 12% as the length of the trombone is varied over a wavelength while the variation of directivity corrected power measurements (black) is smaller but still pronounced. This is because Q_T is sensitive to both directivity and circulator reflections. The inverse transfer function measurements (red) are much less sensitive to trombone length.

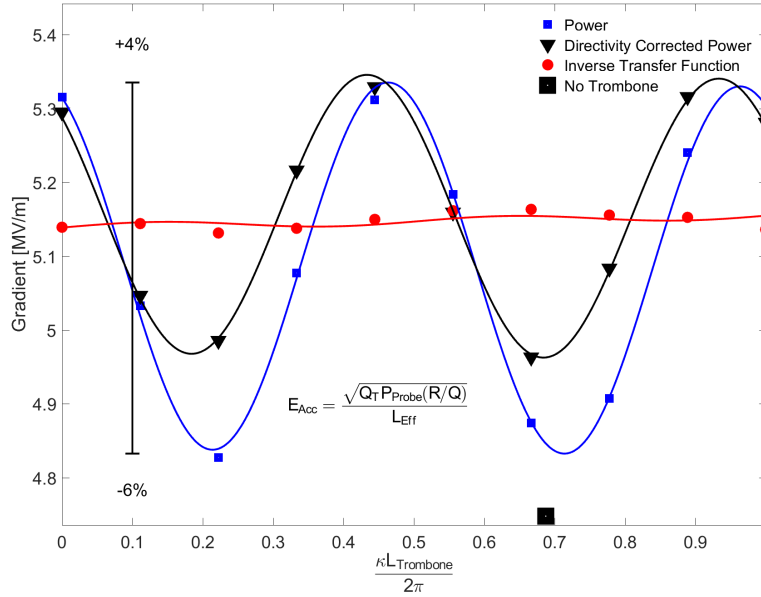


Figure 9: Measured Gradient via Power measurements versus trombone angle with uncorrected signals (Blue Squares) and directivity-corrected signals (Black Triangles) compared to directivity-corrected Transfer Functions (Red Circles). Gradient measured without trombone (Black Square) agrees with trombone scan data.

The black square in Figure 8 again shows the equivalent measurement without a trombone installed in the circuit. Again, the value is consistent with the value expected from the trombone measurements when the phase length of the waveguide is the same.

The blue and red points in Figure 9 respectively compare the cavity gradient, E_{Acc} , as a function as a function of trombone position both before and after the cavity power measurements were corrected for directivity. The red points show the inverse cavity coupling determined using the inverse transfer functions.

The uncorrected power measurements (blue) vary sinusoidally by up to 12% as the length of the trombone is varied over a wavelength while the variation of directivity corrected power measurements (black) is smaller but still pronounced. The inverse transfer function measurements (red) are much less sensitive to trombone length.

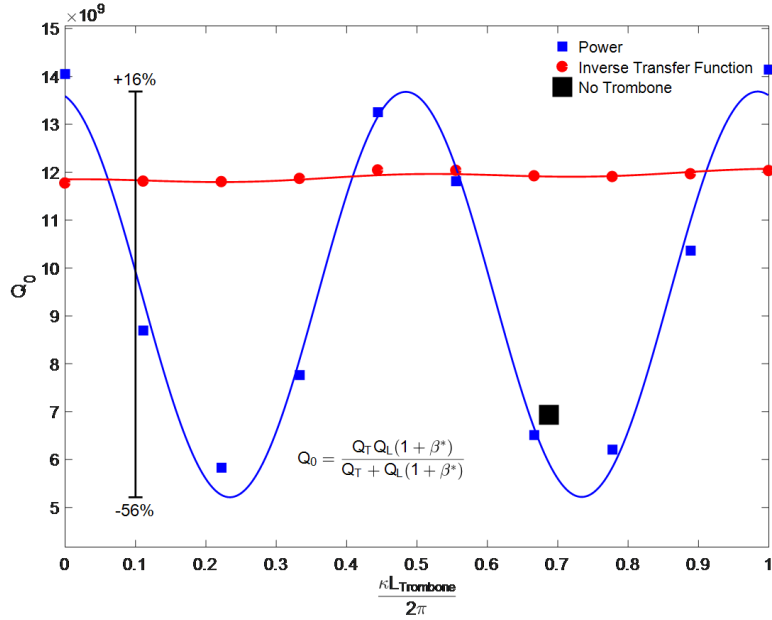


Figure 10: Measured Q_0 via Power measurements versus trombone angle with uncorrected signals (Blue Squares) compared to directivity-corrected Transfer Functions (Red Circles). Q_0 measured without trombone (Black Square) agrees with trombone scan data.

The black square in Figure 9 again shows the equivalent measurement without a trombone installed in the circuit. Again, the value is consistent with the value expected from the trombone measurements when the phase length of the waveguide is the same.

The blue and red points in Figure 10 respectively compare the intrinsic cavity quality factor, Q_0 , as a function of trombone position determined from power measurements to the same quantity determined using the inverse transfer functions.

The power measurements (blue) vary sinusoidally by up to 56% as the length of the trombone is varied over a wavelength while the inverse transfer function measurements (red) are much less sensitive to trombone length.

The black square in Figure 10 again shows the equivalent measurement with no trombone in the circuit. Again, the value is consistent with the value ex-

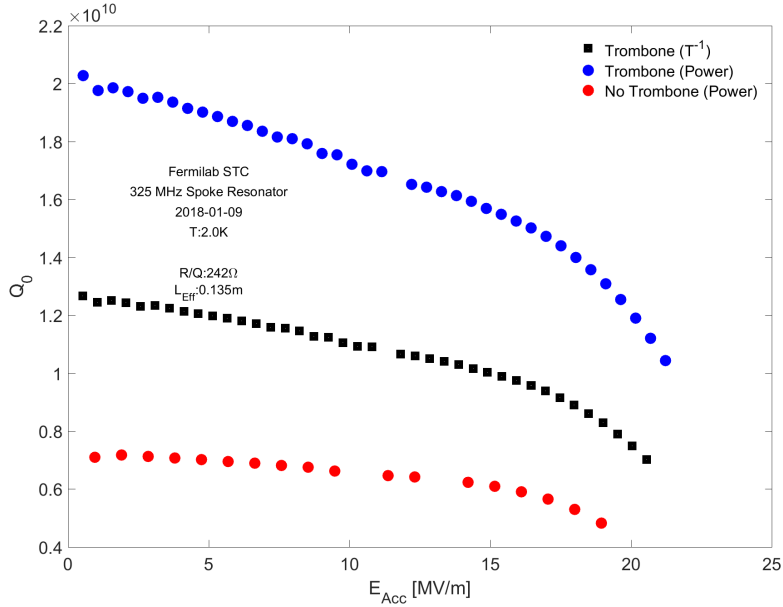


Figure 11: Q_0 versus gradient as measured by power with no trombone (Red Circles), at the initial trombone position which coincides with 'maximum Q_0 ' (Blue Circles), and as measured with directivity-corrected signals via Transfer Functions (Black Squares).

pected from the trombone measurements when the phase length of the waveguide is the same.

Figure 11 shows compares the variation of the intrinsic quality factor with accelerating gradient measured using the power technique with no trombone in the circuit, power technique with the trombone set to zero, and the inverse transfer function technique. The coupling calculated from the power in the cavity RF signals depends strongly on the phase length of the waveguide and cross-talk in the directional coupler. At a trombone length of zero the power-calculated coupling is close 10 at zero gradient while with no trombone the calculated coupling is closer to 4. In comparison, the cavity coupling determined from the inverse transfer functions is much less sensitive to both the phase length of the transmission line and coupler directivity.

6. Acknowledgments

Who?

7. Conclusion

Systematic effects associated with impedance mismatches at the circulator and imperfect directivity limit the accuracy of cavity quality factor measurements if the cavity coupling is not close to critical. Consistency constraints can be used to improve the calibration of the RF signals if the complex base-band signals are recorded in conjunction with a trombone in the circuit. The improved calibration allows accurate measurements to be made over a wider range of couplings.

The intrinsic quality factor calculated from the cavity power signals from a 325 MHz spoke resonator operating at 2K and a nominal gradient of 5 MV/m with a coupling of $\beta^* = 7.14$ showed varied between 5×10^9 and 1.5×10^{10} depending on the phase length of the transmission line driving the cavity.

When calibrated directivity-corrected complex baseband signals were used to determine the inverse transfer functions and the decay time was corrected

for circulator reflections, consistent values for Q_0 of 1.19×10^{10} were obtained independent of the phase length of the waveguide.

- [1] T. Powers, “Theory and Practice of Cavity RF Test Systems”, IAEA-INIS 28.01 (2006).
- [2] J.P. Holzbauer *et al.*, “Systematic uncertainties in RF-based measurement of superconducting cavity quality factors”, Nuclear Instruments and Methods A, 830, 11 September 2016, pp 22-29, 2016.
- [3] M.A. Hassan *et al.*, “Development of Low Single-Spoke Resonators for the Front End of the Proton Improvement Plan-II at Fermilab”, IEEE Transaction on Nuclear Science, Volume 64, Issue 9, September 2017.
- [4] A. Sukhanov *et al.*, “Result of Cold Tests of the Fermilab SSR1 Cavities”, Proceedings of LINAC2014, Geneva, CH, THPP057 (2014).
- [5] M. Chem *et al.*, “Project X superconducting spoke resonator test cryostat 2K conversion”, AIP Conference Proceedings, 1573, 790 (2014).
- [6] J. Branlard *et al.*, “LLRF Design for the HINS-SRF Test Facility at Fermilab”, Proceedings of LINAC2010, Tsukuba, Japan, MOP083 (2010).